JMEPEG (2012) 21:2515–2518
DOI: 10.1007/s11665-012-0269-1

©ASM International
1059-9495/$19.00

Differential Scanning Calorimetric (DSC) Analysis of Rotary Nickel-Titanium (NiTi) Endodontic File (RNEF)

Ray Chun Tung Wu and C.Y. Chung

(Submitted March 3, 2011; in revised form May 6, 2012)

To determine the variation of A_f along the axial length of rotary nickel-titanium endodontic files (RNEF). Three commercial brands of 4% taper RNEF: GTX (#20, 25 mm, Dentsply Tulsa Dental Specialties, Tulsa, OK, USA), K3 (#25, 25 mm) and TF (Twisted File #25, 27 mm) (Sybron Kerr, Orange, CA, USA) were cut into segments at 4 mm increment from the working tip. Regional specimens were measured for differential heat-flow over thermal cycling, generally with continuous heating or cooling (5 °C/min) and 5 min hold at set temperatures (start, finish temperatures): GTX: −55, 90 °C; K3: −55, 45 °C; TF: −55, 60 °C; using differential scanning calorimeter. This experiment demonstrated regional differences in A_f along the axial length of GTX and K3 files. Similar variation was not obvious in the TF samples. A contributory effect of regional difference in strain-hardening due to grinding and machining during manufacturing is proposed.

Keywords DSC, nickel-titanium, rotary file, shape memory alloy, superelastic

1. Introduction

The invention and testing of NiTi file may be traced back to 1988 (Ref 1), while rotary nickel-titanium (NiTi) endodontic file (RNEF) becomes commercially available to the market in 1993 (Ref 2). In dentistry, highly flexible RNEF is considered as an efficient cutting tool which can negotiate readily in the curved root canals. By virtue of its superelasticity, RNEF is highly flexible, exhibiting a larger elastic limit (6-8% strain) (Ref 3) compared to that of conventional stainless steel hand file (0.1-0.2% strain). RNEF surpasses stainless steel hand file in terms of efficiency (Ref 4, 5), reducing procedural errors (Ref 4), and clinical outcome (Ref 4, 5).

The superelastic working temperature of RNEF is thermodynamically limited to within approximately 20 K above its austenitic-finish transformation temperature (A_f) (Ref 6). Although some DSC thermal analyses of RNEF had been reported (Ref 7-13), regional A_f characterization along the axial length of RNEF was not available. Since the fatigue and fracture behavior of superelastic NiTi alloy depends substantially on the A_f transition temperature, we believe that the variation of A_f along the axial length of RNEF should be critical to its performance and life expectancy. It is the purpose of this paper to provide detail transformation temperature measurements for the exploration of the regional variation of A_f along the axial length of selected brands of RNEF commercially available. We want to gain a preliminary understanding of whether such variation in A_f should be considered as a crucial and important factor for the analysis and prediction of fracture behavior of various superelastic RNEFs in relation to its clinical performance.

2. Materials and Methods

Three commercially available brands of 4% taper RNEF (Table 1): GTX (#20, 25 mm, Dentsply Tulsa Dental Specialties, Tulsa, OK, USA), K3 (#25, 25 mm) and TF (Twisted File #25, 27 mm) (Sybron Kerr, Orange, CA, USA) were purchased for this study. They were cut into segments at 4 mm increment from the working tip with plier. The last 0.5 mm of each cut-end was etched for 15 min with a 1:4:5 (v/v) mixture of hydrofluoric acid (48% v/v), nitric acid (70% v/v), and distilled water, respectively, to chemically etch away areas of strain-hardening due to plier crimping (Ref 14). RNEF segments were weighted with electronic beam balance (Analytical Plus-OHAUS) before and after chemical etching.

4% taper RNEF were chosen in this study. Unlike the other tested RNEF with 0.25 mm tip diameter, GTX has a tip diameter of 0.20 mm instead because 0.25 mm design is not available for GTX. Similarly, because 25 mm file length is not available for TF with 4% taper and 0.25 mm tip diameter, file length of 27 mm is chosen for TF instead. K3 (Fig. 1) and TF (Fig. 3) has 16 mm of fluted working length, and the full length were divided into five zones, namely: (A) end tip, (B) near tip, (C) lower body, (D) upper body, and (E) shaft. GTX (Fig. 2) has 20 mm of fluted working length and the full length was divided into six zones, namely: (A) end tip, (B) near tip, (C) lower body, (D) mid-body, (E) upper body, and (F) shaft.

Regional specimens were encased in aluminum pan without crimping, and measured for heat-flow against empty reference Al pan over thermal heat-cool cycling, generally with continuous

---

This article is an invited paper selected from presentations at the International Conference on Shape Memory and Superelastic Technologies 2011, held November 6-9, 2011, in Hong Kong, China, and has been expanded from the original presentation.

Ray Chun Tung Wu and **C.Y. Chung**, Department of Physics and Materials Science, City University of Hong Kong, 83 Tat Chee Avenue, Kowloon Tong, Hong Kong SAR, China. Contact e-mails: RCT.Wu@student.cityu.edu.hk and appchung@cityu.edu.hk.

Table 1 DSC results of RNEF A_f values

Manufacturer	Brand name	File length, mm	Tip diameter, mm	Taper, %	A_f values, °C					
					A	B	C	D	E	F
Dentsply Tulsa Dental Specialties, Tulsa, OK, USA	GTX	25	0.20	4	49.50	46.60	47.77	49.55	49.73	55.60
Sybron Kerr. Orange, CA, USA	K3	25	0.25	4	20.45	19.27	18.27	17.51	21.32	N/A
Sybron Kerr, Orange, CA, USA	Twisted File (TF)	27	0.25	4	17.28	17.62	17.84	17.56	17.65	N/A

(A to F refer to regions of the file shown in Fig. 1 to 3)

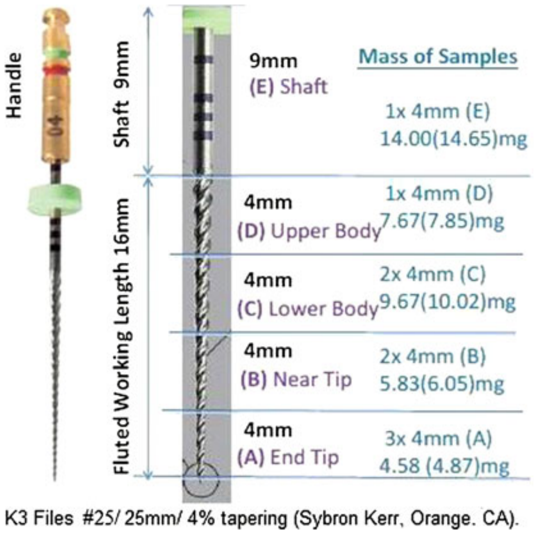

Fig. 1 Diagram of K3 (Ref 18) showing number and mass of regional segments tested (mass before chemical etching is bracketed next to that after etching)

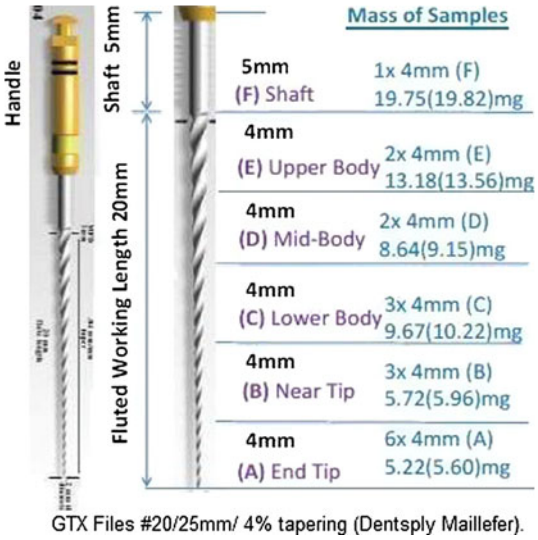

Fig. 2 Diagram of GTX (Ref 17) showing number and mass of regional segments tested (mass before chemical etching is bracketed next to that after etching)

heating or cooling (5 °C/min) and 5 min hold at set temperatures (start, finish temperatures) deduced from pilot studies: GTX: −55, 90 °C; K3: −55, 45 °C; TF: −55, 60 °C; by using thermal analysis (TA) differential scanning calorimeter (DSC) (TA2910) calibrated with indium and mercury. DSC chamber was purged with nitrogen gas at a flow rate of 50 mL/min. Data were analyzed by software (Universal Analysis). A_f values were determined from the heat-flow versus temperature plot by locating the intersection of the tangent of the steepest endothermic slope at the austenitic-end with the baseline extension of the heating curve according to ASTM F2004-05 (Ref 15). On the basis of pilot study results on three consecutive DSC cycle measurements, data of the second and third cycle were found to be highly reproducible and match each other closely, thus two consecutive DSC cycles were performed for each specimen, and the data of the second cycle were used for comparison.

3. Results

A total of 42 segments from the three RNEF brands was prepared and tested. One to six segments of the same region for each brand were used for each DSC analysis. The total number and mass of regional segments tested are depicted in Fig. 1 to 3.

The A_f values of K3, GTX, and TF at different regions along the axial length are shown in Table 1. GTX had the overall highest A_f values at all regions along the file length. The end tip A_f values of K3, GTX, and TF were 20.45, 49.50, and 17.28 °C, respectively. Whereas the shaft A_f values of K3, GTX, and TF files were 21.32, 55.60, and 17.65 °C, respectively. From the plots of A_f values against mean distance from working tip (Fig. 4), remarkable drop in A_f values from the shaft to the fluted length was observed for both K3 and GTX. The A_f value for K3 increased gradually along its fluted working length toward the working tip. Whereas the A_f value for GTX decreased gradually along its fluted working length but to increase again on approaching the last 4 mm of working tip. There was, however, no significant difference in the A_f values of TF along the file length (Table 1).

Typical DSC curves of K3, GTX, and TF are shown in Fig. 5, 6, and 7, respectively. A major endothermic peak and exothermic peak were found associated with the heating and cooling curves, respectively. An additional minor but relatively ill-resolved exothermic peak was also spotted at a temperature lower than that of the major peak.

4. Discussion

The results of A_f values suggested that, at room temperature, reversibly transformable martensite have completely returned to its parent austenitic phase both for K3 and TF, and they possess

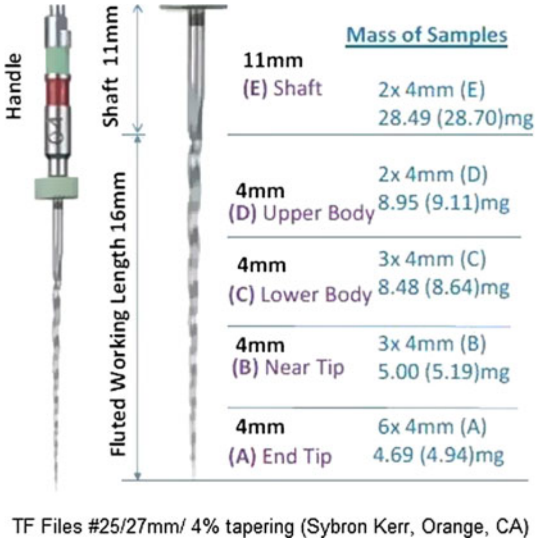

Fig. 3 Diagram of TF (Ref 18) showing number and mass of regional segments tested (mass before chemical etching is bracketed next to that after etching)

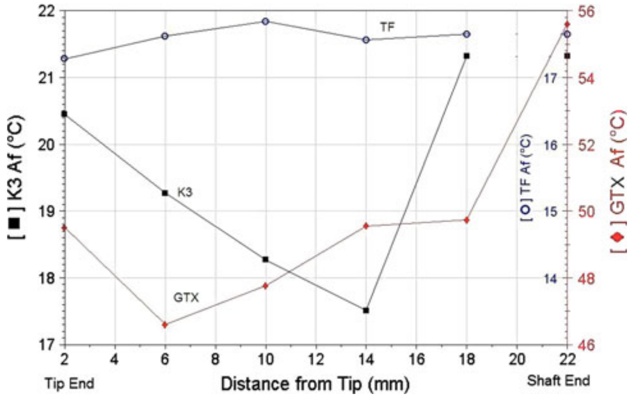

Fig. 4 Plots of A_f values as a function of the mean distance from file tip for K3, GTX, and TF

superelastic character at 37 °C oral temperature, i.e., about 15-20 °C above their corresponding A_f. On the contrary, austenitic transformation from martensite is far from completion for GTX at room temperature, and that at oral temperature below its A_f value, no superelastic character would be activated. While DSC data of the transformation temperature of RNEF have been reported (Ref 7-13), some of these studies were carried out over 5 years ago (Ref 7, 8) and can no longer reliably represent the RNEF products marketed currently. The work of Miyai et al. (Ref 12) found that the A_f value of K3 was 5 °C, which differ remarkably from our present result of 20.45 and 21.32 °C at end tip and shaft, respectively, for K3. We believe that the present K3 should possess better superelastic properties than their earlier products 5 years ago. The difference may be attributed to the changes made by manufacturer to product manufacturing and processing over the years to enable stress-induced superelasticity of RNEF to manifest at oral temperature, thus making their product more endurable to mechanical cycling fatigue.

Among the RNEF chosen for this study, GTX and TF belong to products of latest development featuring M-wire technology and R-phase technology, respectively (Ref 16).

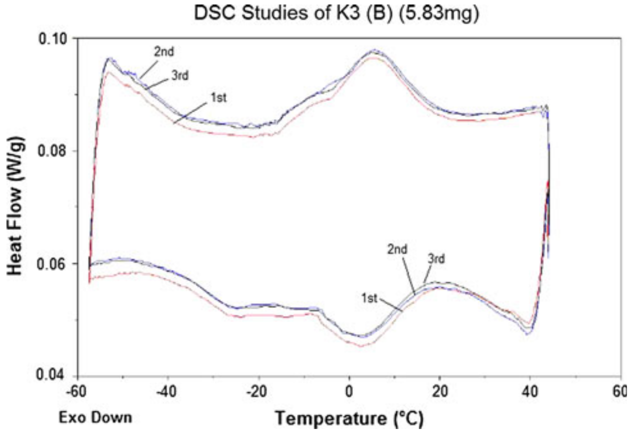

Fig. 5 DSC (three consecutive cycles) curves of K3 at near-tip region with a (2-segment) sample mass of 5.83 mg after chemical etching

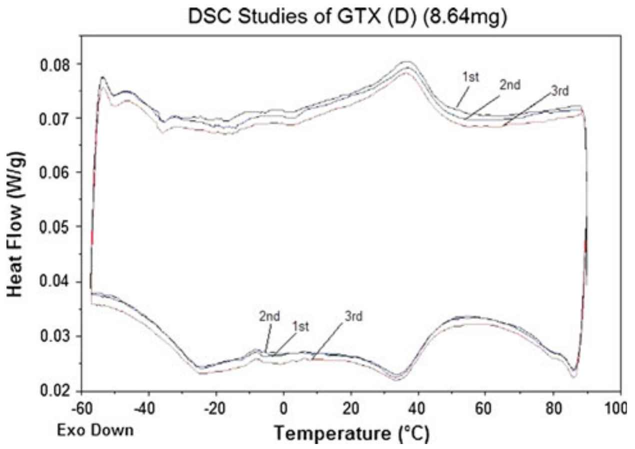

Fig. 6 DSC (three consecutive cycles) curves of GTX at mid-body region with a (2-segment) sample mass of 8.64 mg after chemical etching

According to manufacturer, M-wire technology involves precise control of alloy temperatures and tensile treatments during manufacturing with resultant increase in the flexibility and resistance of file to cyclic fatigue (Ref 17). Whereas R-phase heat treatment technology makes use of heating and cooling protocols to produce fine R-phase crystalline structure thus enabling one-piece twisting of blank wire into triangular cross section (Ref 18) without the conventional need of grinding machining of flutes for RNEF like that of K3 and GTX (Ref 9, 19) from starting wire blanks.

Shen et al. (Ref 13) reported the A_f values for segments close to the shaft of TF and ProFile Vortex (M-wire) to be 17.62 and 50.4 °C, respectively, which are in good agreement with our results of 17.56 and 49.55 °C for corresponding regions of TF and GTX (M-wire). Nevertheless, GTX and ProFile Vortex should not be considered identical even though they are M-wire rotary file manufactured by the same company.

We find that regional difference in A_f values is present for K3 and GTX files but not for TF. This can possibly be due to the contributory effect of regional difference in strain-hardening caused by grinding and machining during the manufacturing process of RNEF NiTi materials. This is in agreement with the observation of differences in DSC measurements between starting wire blanks and machined RNEF in the work of Brantley et al. (Ref 8). The significance of the effect of

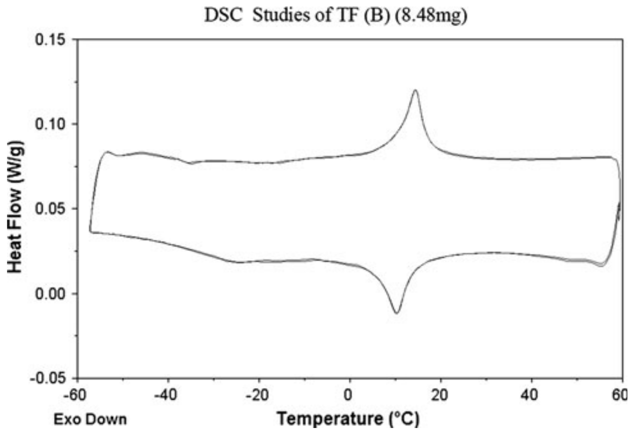

Fig. 7 DSC (two consecutive cycles) curves of TF at near-tip region with a (3-segment) sample mass of 8.48 mg after chemical testing

processing on fatigue properties of NiTi has been reviewed and highlighted by Pelton (Ref 20). Eliminating the need for machining flutes and hence minimizing the associated surface defects for RNEF (Ref 21, 22) may be an advantage as far as the resistance to initiation of fatigue failure is concerned.

The fact that regional variation in A_f values can occur with some RNEF is a challenge to researchers in preparing for representative database for the transformation temperatures of RNEF. On top of the need to update DSC data reported for RNEF in the past to watch out for hidden latest changes in NiTi alloy composition or thermomechanical treatment by manufacturers, a more realistic and accurate approach to A_f determination using DSC measurements for RNEF, while taking into account of the regional variation of A_f values, and the subsequent superelastic properties, should be adopted to enable better understanding and prediction of the high strain fatigue fracture of RNEF in relation to its clinical performance. We are making arrangement in correlating the A_f transition temperature and the fracture behavior of these RNEF. The experimental result and analysis will be reported very soon.

5. Conclusion

Among the three commercial brands of 4% taper RNEF studied: GTX (#20, 25 mm, Dentsply Tulsa Dental Specialties, Tulsa, OK, USA), K3 (#25, 25 mm) and TF (Twisted File #25, 27 mm) (Sybron Kerr, Orange, CA, USA), only the latter two sets of samples possess superelastic character at room temperature and oral temperature. Regional difference in A_f values is observed for K3 and GTX but not for TF. A contributory effect of regional difference in strain-hardening due to grinding and machining during manufacturing is proposed. A more realistic approach to DSC measurements of RNEF, while taking into account of the regional variation in A_f values, should be adopted to allow for better interpretation of the superelastic properties of RNEF in relation to its clinical performance and high strain fatigue behavior.

Acknowledgment

This paper was financially supported by the CityU SRG Grant # 7002691.

References

1. H.M. Walia, W.A. Brantley, and H. Gerstein, An Initial Investigation of the Bending and Torsional Properties of Nitinol Root Canal Files, *J. Endod.*, 1988, **14**, p 346–351
2. O.A. Peters, *Rotary Instrumentation: An Endodontic Perspective, Endodontics: Colleagues for Excellence Newsletter*, American Association of Endodontists, Chicago, Winter 2008, pp. 1–6. www.aae.org/uploadedFiles/Publications_and_Research/Endodontics_Colleagues_for_Excellence_Newsletter/winter08ecfe.pdf
3. A.L. McKelvey and R.O. Ritchie, Fatigue-Crack Growth Behavior in the Superelastic and Shape-Memory Alloy Nitinol, *Met. Mater. Trans. A*, 2001, **32A**, p 731–743
4. Y. Shen, J.M. Coil, and M. Haapasalo, Defects in Nickel-Titanium Instruments After Clinical Use. Part 3: A 4-Year Retrospective Study from an Undergraduate Clinic, *J. Endod.*, 2009, **35**, p 193–196
5. C.H. Fleming, M.S. Litaker, L.W. Alley, and P.D. Eleazer, Comparison of Classic Endodontic Techniques Versus Contemporary Techniques on Endodontic Treatment Success, *J. Endod.*, 2010, **36**, p 414–418
6. Y. Liu and S.P. Galvin, Criteria for Pseudoelasticity in Near-Equiatomic NiTi Shape Memory Alloys, *Acta Mater.*, 1997, **45**, p 4431–4439
7. G. Kuhn and L. Jordan, Fatigue and Mechanical Properties of Nickel-Titanium Endodontic Instruments, *J. Endod.*, 2002, **28**, p 716–720
8. W.A. Brantley, T.A. Svec, M. Iijima, J.M. Powers, and T.H. Grentzer, Differential Scanning Calorimetric Studies of Nickel Titanium Rotary Endodontic Instruments after Simulated Clinical Use, *J. Endod.*, 2002, **28**, p 774–778
9. S. Zinelis, T. Eliades, and G. Eliades, A Metallurgical Characterization of Ten Endodontic Ni-Ti Instruments: Assessing the Clinical Relevance of Shape Memory and Superelastic Properties of Ni-Ti Endodontic Instruments, *Int. Endod. J.*, 2010, **43**, p 125–134
10. G. Alexandrou, K. Chrissafis, L. Vasiliadis, E. Pavlidou, and E.K. Polychroniadis, Effect of Heat Sterilization on Surface Characteristics and Microstructure of Mani NRT Rotary Nickel-Titanium Instruments, *Int. Endod. J.*, 2006, **39**, p 770–778
11. G.B. Alexandrou, K. Chrissafis, L.P. Vasiliadis, E. Pavlidou, and E.K. Polychroniadis, SEM Observations and Differential Scanning Calorimetric Studies of New and Sterilized Nickel-Titanium Rotary Endodontic Instruments, *J. Endod.*, 2006, **32**, p 675–679
12. K. Miyai, A. Ebihara, Y. Hayashi, H. Doi, H. Suda, and T. Yoneyama, Influence of Phase Transformation on the Torsional and Bending Properties of Nickel-Titanium Rotary Endodontic Instruments, *Int. Endod. J.*, 2006, **39**, p 119–126
13. Y. Shen, H.M. Zhou, Y.F. Zheng, L. Campbell, B. Peng, and M. Haapasalo, Metallurgical Characterization of Controlled Memory Wire Nickel-Titanium Rotary Instruments, *J. Endod.*, 2011, **37**, p 1566–1571
14. B.R. Hilt, C.J. Cunningham, C. Shen, and N. Richards, Torsional Properties of Stainless-Steel and Nickel-Titanium Files After Multiple Autoclave Sterilizations, *J. Endod.*, 2000, **26**, p 76–80
15. Standard Test Method for Transformation Temperature of Nickel-Titanium Alloys by Thermal Analysis, ASTM F2004-05
16. C.M. Larsen, I. Watanabe, G.N. Glickman, and J.N. He, Cyclic Fatigue Analysis of a New Generation of Nickel Titanium Rotary Instruments, *J. Endod.*, 2009, **35**, p 401–403
17. GTX rotary endodontic file: manufacturer's web site. http://www.dentsply.co.uk
18. TF rotary endodontic file: manufacturer's web site. http://www.sybronendo.com
19. S.A. Thompson, An Overview of Nickel-Titanium Alloys used in Dentistry, *Int. Endod. J.*, 2000, **33**, p 297–310
20. A.R. Pelton, Nitinol Fatigue: A Review of Microstructures and Mechanisms, *JMEPEG*, 2011, **20**, p 613–617
21. S.B. Alapati, W.A. Brantley, T.A. Svec, J.M. Powers, and J.C. Mitchell, Scanning electron Microscope Observations of New and Used Nickel-Titanium Rotary Files, *J. Endod.*, 2003, **29**, p 667–669
22. S.B. Alapati, W.A. Brantley, T.A. Svec, J.M. Powers, J.M. Nusstein, and G.S. Daehn, SEM Observations of Nickel-Titanium Rotary Endodontic Instruments that Fractured During Clinical Use, *J. Endod.*, 2005, **31**, p 40–43